Switching on Fast Lithium Ion Conductivity in Garnets: The Structure and Transport Properties of $Li_{3+x}Nd_3Te_{2-x}Sb_xO_{12}$

Michael P. O'Callaghan,[†] Andrew S. Powell,[†] Jeremy J. Titman,[†] George Z. Chen,[‡] and Edmund J. Cussen*,[§]

The School of Chemistry and The School of Chemical, Environmental and Mining Engineering, The University of Nottingham, Nottingham, United Kingdom NG7 2RD, WestCHEM, The Department of Pure and Applied Chemistry, The University of Strathclyde, Glasgow, United Kingdom G1 1XL

Received December 24, 2007

Polycrystalline samples of the garnets $Li_{3+x}Nd_3Te_{2-x}Sb_xO_{12}$ have been prepared by high temperature solid state synthesis. X-ray and neutron powder diffraction data show that all compounds crystallize in the space group $Ia\bar{3}d$ with lattice parameters in the range 12.55576(12) Å for $x = 0.05$ to 12.6253(2) Å for $x = 1.5$. The lithium is distributed over a mixture of oxide tetrahedra and heavily distorted octahedra. Increasing the lithium content in these compounds leads to the introduction of vacancies onto the tetrahedral position and an increasing concentration of lithium found in the octahedra. The latter exhibit considerable positional disorder with two lithium cations positions within each octahedron. Impedance measurements show fast ion conduction with an activation energy of ca. 0.59(6) eV that is largely invariant with composition. Solid-state Li NMR measurements indicate that there is no exchange of lithium between the different coordination environments. These results indicate that lithium conduction in the garnet structure occurs exclusively via a network of edge-linked distorted oxide octahedra and that the tetrahedrally coordination lithium plays no part in the transport properties.

Introduction

Rechargeable lithium batteries currently use polymer-based materials as electrolytes.[1,2] While these provide the necessary Li^+ mobility, there are flammability, toxicity, and leakage problems associated with these materials that are driving the search for safer replacements.[3] Crystalline ceramic solids that contain mobile lithium ions have the potential to combine the ionic mobility of a liquid with the attractive mechanical properties of a robust and chemically inert solid and for this reason are favored alternatives to polymer electrolytes. Unfortunately, most candidate materials have features that make them unsuitable for use under the operational conditions of a secondary lithium battery such as air/moisture sensitivity, appreciable electronic conductivity or chemical instability. A key problem has been finding suitable electrolytes that are capable of resisting the highly reducing environment of a secondary battery; for example while $Li_{3x}La_{2/3-x}TiO_3$ shows the highest lithium mobility of any crystalline solid, $\sigma_{RT} \approx 1 \times 10^{-3}$ S cm^{-1}, this material undergoes reductive insertion of Li^+ when in contact with elemental lithium leading to increased electrical conductivity[4,5] and self-discharge of the cell. Lithium garnets based on the d^0 cations Ta^{5+} and Nb^{5+} show negligible electronic conductivity, are chemically unreactive toward metallic lithium, are stable in air at temperatures up to 600 °C and show lithium conductivity of up to 1×10^{-5} S cm^{-1} at room temperature.[6–8] These features make them candidates to replace polymer-based electrolytes in safety-critical applications, such as biomedical implants, where no suitable crystalline material has yet been identified. Despite a number of studies[7,9–11] the nature of the path for lithium conduction in these phases remains a subject of speculation. Here we report a comprehensive study of the structure and ion transport properties of a series of garnets that unambiguously establish the nature of the mobile species and the pathway for ion transport in this structure.

The garnet structure can be illustrated with reference to the prototypical grossular structure of $Ca_3Al_2Si_3O_{12}$, which contains a mixture of square antiprismatic, octahedral and tetrahedral coordination environments in a 3:2:3 ratio.[12] Lithium containing garnets that follow this cation ratio fill the tetrahedral site with Li^+ giving a stoichiometry such as $Li_3Nd_3Te_2O_{12}$ where Nd^{3+} and Te^{6+} fill the 8-coordinate and

* Corresponding author. E-mail: edmund.cussen@strath.ac.uk.
[†] The School of Chemistry, The University of Nottingham.
[‡] The School of Chemical, Environmental and Mining Engineering, The University of Nottingham.
[§] The University of Strathclyde.

(1) Tarascon, J.-M.; Armand, M. *Nature* **2001**, *414*, 359–367.
(2) Christie, A. M.; Lilley, S. J.; Staunton, E.; Andreev, Y. G.; Bruce, P. G. *Nature* **2005**, *433*, 50–53.
(3) Tobishima, S.; Yamaki, J. *J. Power Sources* **1999**, *81–82*, 880.
(4) Stramare, S.; Thangadurai, V.; Weppner, W. *Chem. Mater.* **2003**, *15* (21), 3974–3990.
(5) Yashima, M.; Itoh, M.; Inaguma, Y.; Morii, Y. *J. Am. Chem. Soc.* **2005**, *127*, 3491–3495.
(6) Thangadurai, V.; Kaack, H.; Weppner, W. J.F. *J. Am. Ceram. Soc.* **2003**, *86* (3), 437–440.
(7) Thangadurai, V.; Weppner, W. *Adv. Funct. Mater.* **2005**, *15* (1), 107–112.
(8) Thangadurai, V.; Weppner, W. *J. Power Sources* **2005**, *142*, 339–344.
(9) Thangadurai, V.; Adams, S.; Weppner, W. *Chem. Mater.* **2004**, *16*, 2998–3006.
(10) O'Callaghan, M. P.; Cussen, E. J. *Chem. Commun.* **2007**, 2048–2050.
(11) van, Wüllen, L.; Echelmeyer, T.; Meyer, H.-W.; Wilmer, D. *Phys. Chem. Chem. Phys.* **2007**, *9*, 3298.
(12) Abrahams, S. C.; Geller, S. *Acta Crystallogr.* **1958**, *11*, 437.

10.1021/cm703677q CCC: $40.75
Published on Web 03/05/2008

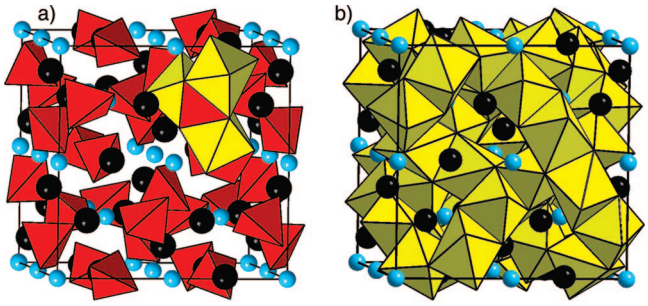

Figure 1. Representation of the structures of the garnets $Li_3Nd_3Te_2O_{12}$ and $Li_5La_3Ta_2O_{12}$. Black and blue spheres represent Ln^{3+} and Te/Ta, respectively. In $Li_3Nd_3Te_2O_{12}$, lithium exists solely in tetrahedral coordination as indicated by red units as shown in (a). In $Li_5La_3Ta_2O_{12}$, the additional lithium occupies heavily distorted octahedral sites, illustrated by yellow octahedra, that cap each face of the LiO_4 tetrahedra as illustrated for a portion of the structure in (a). For clarity, only three such sites are shown; in practice, each red tetrahedral unit is capped by four face-sharing octahedral sites, leading to a continuous framework of edge-sharing LiO_6 units as shown in (b).

octahedral sites respectively. This compound shows negligible ionic conductivity below 400 °C and activated charge transport above this temperature[13] with a relatively large activation energy of 1.34(2) eV. This behavior indicates a different mechanism to that reported in the fast Li^+ conducting phases such as $Li_5La_3Ta_2O_{12}$, $Li_5La_3Nb_2O_{12}$,[6] $Li_6BaLa_2Nb_2O_{12}$, and $Li_6BaLa_2Ta_2O_{12}$[7] where the activation energies are in the range 0.4 ev $\leq E_a \leq$0.6 ev and fast Li^+ conduction occurs at room temperature. It is clear that in these highly conducting phases the cation concentration is larger than permitted by the conventional garnet stoichiometry; indeed the lithium concentration in the garnet structure can be increased to yield a compound of stoichiometry $Li_{6.6}Ba_{1.6}La_{1.4}Ta_2\ O_{12}$.[10] In such cation-rich phases the tetrahedral site contains 20–40% vacancies with the excess lithium partially occupying an additional coordination site, shown in Figure 1, that is normally vacant in the garnet structure. This heavily distorted octahedral site is linked to the tetrahedral position via a shared oxide face and in the limiting composition $Li_{6.6}Ba_{1.6}La_{1.4}Ta_2O_{12}$ both of these sites are occupied simultaneously giving a remarkably short Li···Li distance of 2.47(1) Å.[10]

In situ neutron diffraction experiments on $Li_5La_3Ta_2O_{12}$[14] and $Li_6BaLa_2Ta_2O_{12}$[10] have shown that there is negligible variation in the lithium distribution across the tetrahedral and octahedral interstices on heating the samples from room temperature to 600 °C. No variation in properties have been reported as a function of synthesis conditions and the smooth evolution of lithium distribution observed[10] in the series $Li_{5+x}Ba_xLa_{3-x}Ta_2O_{12}$ and the similarity of lithium occupancies reported in $Li_5La_3M_2O_{12}$ (M = Ta, Nb,[14] Sb[15]) and $Li_6BaLa_2Ta_2O_{12}$[10] and $Li_6SrLa_2Nb_2O_{12}$[16] suggests that the lithium distribution observed in these compounds is the equilibrium value. The observation of positional disorder in the lithium in the oxide octahedra has suggested that these lithium species are mobile. However, it has been noted that the disorder observed in diffraction experiments is indicative of static displacements and the data provide no direct evidence of ion mobility.[14] Conductivity measurements have shown that significant changes in site occupancies have no substantial impact on conductivity suggesting that the ion mobility is not a straightforward function of the distribution of lithium over tetrahedral and octahedral sites.[16]

A recent Li NMR study of $Li_5La_3Nb_2O_{12}$ indicated the presence of two lithium sites in the material which showed different mobilities and no exchange of lithium between these positions leading the authors to conclude that cations occupying only one of the two lithium positions is mobile.[11] This mobility was assigned to the octahedral sites in the structure. However, the NMR data indicated a large variation in the fractions of lithium on the two sites that is incompatible with the values of 82(2) and 41(1)% consistently observed across multiple samples by different research groups for $Li_5La_3M_2O_{12}$ (M = Ta, Nb, Sb) at temperatures between 2 and 873 K.[14] On the basis of the NMR data, it was concluded that a sample prepared at 1123 K contained immobile lithium at room temperature, whereas preparation at 1173 K resulted in a sample with highly mobile lithium under ambient conditions. This observation is inconsistent with the report in related garnets[17] of a variation in conductivity of no more 1 order of magnitude as a result of variable sintering temperatures. Moreover, this variation was ascribed to the effect of changes in microstructure of the samples during the synthesis. It is not clear if the lithium exchange observed in the NMR data is associated with overall ion migration, or simply movement of a single lithium ion between the three distinct cation positions within the distorted oxide that have been identified by neutron diffraction experiments.[14,16] The latter situation would go some way toward explaining the discrepancy between the ion mobilities inferred from the NMR data and that observed via bulk measurements.

The behavior of lithium in the garnet structure that has been observed thus far can be divided into two types: (i) where the conventional garnet stoichiometry is followed the tetrahedral site is full, the distorted octahedral site is empty and limited conductivity results and; (ii) in the cation-rich phases $Li_{5+x}A_xLa_{3-x}M_2O_{12}$ (A = Ca, Sr, Ba and M = Ta, Nb, Sb) lithium and vacancies are disordered over both the octahedral and tetrahedral sites resulting in room temperature ion conductivity with evidence from NMR that a substantial portion of lithium is immobile in the structure. From these studies it is becoming clear that a wide range of techniques need to be used to develop a mechanism of ion mobility in the garnet structure; namely neutron diffraction in order to establish the average (crystallographic) lithium ion distribution, Li NMR to examine both the local lithium distribution and to probe the mobility between sites and bulk transport measurements to determine whether local ion movement leads to bulk charge transport, rather than hopping between sites within a single distorted oxide octahedron. To date no studies have applied more than one of these three techniques to fast ion conducting garnets.

(13) O'Callaghan, M. P.; Lynham; D. R.; Chen, G. Z.; Cussen, E. J. *Chem. Mater.* **2006**, *18* (19), 4681–4689.
(14) Cussen, E. J. *Chem. Commun.* **2006**, 412–413.
(15) Cussen, E. J.; Yip, T. W. S. *J. Solid State Chem.* **2007**, *180*, 1832–1839.
(16) Percival, J.; Slater, P. R. *Solid State Commun.* **2007**, *142* (6), 355–357.
(17) Isasi, J.; Veiga, M. L.; Saez-Puche, R.; Jerez, A.; Pico, C. *J. Alloys Compd.* **1991**, *177*, 251–257.

To determine the nature of the site that provides Li^+ mobility in garnets we decided to study a series of compounds that bridge the gap between these two behavioral classes. To this end we have prepared a series of compounds $Li_{3+x}Nd_3Te_{2-x}Sb_xO_{12}$ where the substitution of Te^{6+} by Sb^{5+} is used to drive the incorporation of additional lithium into the structure of the end member $Li_3Nd_3Te_2O_{12}$ and thus increase the lithium concentration beyond the three lithium per formula that can be accommodated on the tetrahedral site in the structure. The resultant compounds have been structurally characterized by X-ray and neutron diffraction and solid-state ^6Li and ^7Li NMR. The latter also provides information on the dynamic behavior of lithium and this is complemented by variable temperature impedance spectroscopy measurements that provide an assessment of the bulk ionic mobility in these materials. By using this range of techniques to probe these materials we aim to provide a conclusive description of the mobile species in these lithium-conducting compounds and thus provide the information necessary to advance the optimization of this important property in the garnet structure.

Experimental Section

Polycrystalline samples of $Li_{3+x}Nd_3Te_{2-x}Sb_xO_{12}$ ($0.05 \leq x \leq 1.5$) were prepared via solid-state ceramic routes. Stoichiometric quantities of lithium carbonate, dried neodymium oxide, tellurium(IV) oxide, and antimony(III) oxide were ground, pressed into pellets, and heated in air from room temperature to 700 at 1 °C min^{-1} and held at this temperature for 7 h. This was followed by several additional grinding and heating steps (850 °C $\leq T \leq$ 960 °C) for between 10 and 60 h per step, with the addition of excess Li_2CO_3 at several intervals to compensate for loss of lithium as Li_2O. The progress of the syntheses was monitored by X-ray powder diffraction and was stopped when the diffraction pattern could be indexed as arising from a cubic phase, $a \approx 12.6$ Å, indicative of a garnet. X-ray diffraction data suitable for Rietveld refinement were collected from the resultant materials in the range $12° \leq 2\theta \leq 80°$ using a Philips Xpert diffractometer operating using Cu Kα radiation.

Neutron powder diffraction data were collected from samples prepared using $^7Li_2CO_3$ ($^7Li \geq 99\%$, $b_{len} = -2.22$ fm) in order to minimize the absorption due to ^6Li nuclei and provide the maximum contrast with the other nuclei. Measurements were performed at the ISIS facility, Rutherford-Appleton laboratories, using three detector banks of the time-of-flight instrument Polaris to collect data in the range 0.8 Å $\leq d \leq$ 8.0 Å. Data were corrected for absorption using the CORRECT routine within the GENIE suite of programs. Neutron diffraction data were also collected using the constant wavelength D1A diffractometer at the Institut Laue Langevin, Grenoble. Rietveld refinement was performed on all data sets using the GSAS suite of programs.[18] A convolution of exponential and pseudo-Voigt functions were used to describe the peak shape of data collected from Polaris and a pseudo-Voigt function modeled the peak shapes of the diffraction profiles collected from D1A and the laboratory X-ray diffractometer.

Solid-state ^6Li and ^7Li MAS NMR spectra were recorded at Larmor frequencies of 44.2 and 116.6 MHz, respectively, using 3.2 mm rotors spinning at typically 20 kHz. A spin–echo pulse sequence was used with $\pi/2$ pulse lengths of 2 μs and an echo time of typically 50 μs, so that the sequence was synchronized with the spinning. The acquisition time was 4 ms, and the dwell time was 1 μs.

For quantitative measurements, relaxation delays as long as 3600 s were necessary to avoid saturation. The time domain signals were left shifted to the echo maximum and Fourier transformed with no additional line-broadening. The resulting spectra were fitted to a set of Gaussian lines to extract linewidths and intensities. Additional experiments were carried out at temperatures up to 473 K. Resonance shifts are referenced to 1 mol dm^{-3} aqueous LiCl.

Transport measurements were performed on circular pellets with a diameter of 10 mm, a thickness at 2–3 mm and a density of ca. 3.6 g cm^{-3}. The pellets were prepared using natural abundance lithium carbonate. The pellet was first sintered at 700 °C in air and platinum wire was subsequently adhered to each face of the pellet using platinum conductive paint which acts as a blocking electrode to lithium ions. The measurements were performed inside a gastight glass tube under flowing dry air using a frequency response analyzer in the range 1 Hz to 70 kHz, operating with a voltage of 0.35 V. In each experiment, the pellet was heated to 600 °C and cooled to room temperature in order to cure the paint. This was followed by multiple heating and cooling cycles in the temperature range 25 °C $\leq T \leq$ 600 °C, with data points recorded under isothermal conditions after allowing the sample to equilibrate for 2 h at each temperature. Each data set displayed minimal time dependence of the impedance behavior, with all systems showing repeatable results after the first 10–20 min at each temperature. The Autolab V4.9 suite of programs was used to collect and analyze the data.

Results

Crystallographic Structure. Initial analysis of X-ray diffraction data collected from $Li_{3+x}Nd_3Te_{2-x}Sb_xO_{12}$ proceeded by comparison with known phases. The $x = 0$ compound $Li_3Nd_3Te_2O_{12}$ adopts the conventional garnet structure in the space group $Ia\bar{3}d$ and the $x = 2$ end member $Li_5Nd_3Sb_2O_{12}$ has been reported in the space group $I2_13$.[17] However it has recently been shown[15] that the assignment of this space group to the related phase $Li_5La_3Sb_2O_{12}$ underestimated the true symmetry, $Ia\bar{3}d$. Careful inspection of the X-ray diffraction data collected from all compounds in the $Li_{3+x}Nd_3Te_{2-x}Sb_xO_{12}$ series revealed the reflection conditions $0kl$: $k,l = 2n$, hhl: $2h+l = 4n$, $h00$: $h = 4n$ that are uniquely associated with $Ia\bar{3}d$. Consequently, all data were analyzed in this space group.

The end member $Li_3Nd_3Te_2O_{12}$ contains lithium exclusively on the tetrahedral (24*d*) site. However, the site symmetry of this position does not allow for more than three lithium per formula unit; therefore, for compositions $x > 0$, the increased lithium content must lead to population of a crystallographic site that is unoccupied in $Li_3Nd_3Te_2O_{12}$. Previous studies on $Li_{5+x}Ba_xLa_3Ta_2O_{12}$[10] show that increasing lithium content leads to a depopulation of the 24*d* site accompanied by a corresponding increase in octahedral site occupancy. For $Li_{3+x}Nd_3Te_{2-x}Sb_xO_{12}$, it was anticipated that similar occupational disorder across these octahedrally- and tetrahedrally coordinated sites may occur. High resolution neutron powder diffraction data were collected from $Li_{3+x}Nd_3Te_{2-x}Sb_xO_{12}$ ($x = 0.5, 1$) in order to determine the exact lithium environment.

Initial investigation of the lithium distribution in this series proceeded by analysis of the data collected from

(18) Larson, A. C.; von Dreele, R. B. *General Structure Analysis System (GSAS)*; Los Alamos National Laboratories: Los Alamos, NM, 1990.

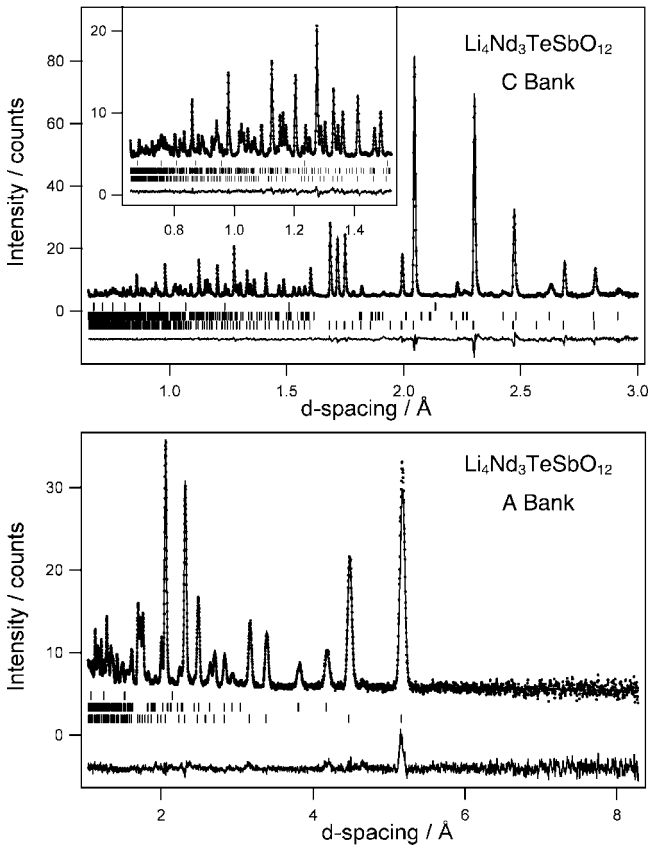

Figure 2. Observed (dots), calculated (line), and difference neutron diffraction patterns obtained from $Li_4Nd_3TeSbO_{12}$. The inset in the upper trace shows the quality of fit obtained at small *d*-spacings. Markers indicate allowed Bragg reflections arising from the garnet (bottom), lithium carbonate impurity (middle), and the vanadium sample holder (top).

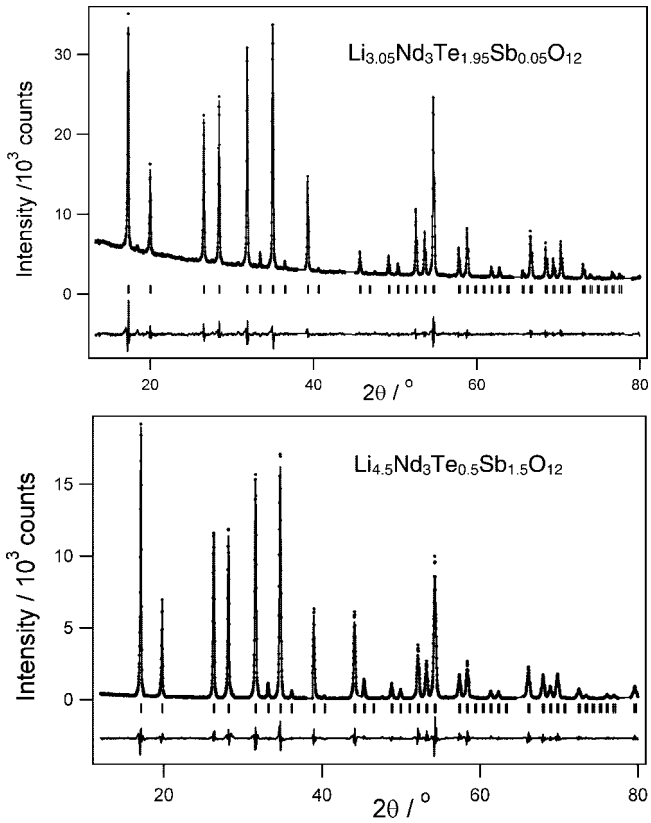

Figure 3. Observed (dots), calculated (line), and difference X-ray diffraction patterns of $Li_{3.05}Nd_3Te_{1.95}Sb_{0.05}O_{12}$ and $Li_{4.5}Nd_3Te_{0.5}Sb_{1.5}O_{12}$. Markers indicate the positions of allowed reflections. Excluded regions were contaminated with peaks arising from the aluminium sample holder.

$Li_4Nd_3TeSbO_{12}$. These data were modeled using a starting structure which contained lithium distributed over the 24*d* sites and a 48*g* position near the center of the octahedron. The occupancies of these two positions were allowed to vary within the constraint imposed by stoichiometry. The refinement proceeded to convergence but resulted in displacement parameters of the octahedrally coordinated lithium cations that were over an order of magnitude greater than typically found in a crystalline solid. In order to account for this positional disorder the lithium occupying the distorted octahedron was modeled using a general position, 96*h*, that generates two lithium species per octahedron. This readily refined to convergence and permitted refinement of the atomic coordinates of this lithium position to yield the high-quality fit to the diffraction data shown in Figure 2. The final structural model employed a single displacement parameter to describe the behavior of the lithium cations and used an anisotropic description of the displacement of all other ions. The data collected from $Li_{3.5}Nd_3Te_{1.5}Sb_{0.5}O_{12}$ were modeled in the same way but the coordinates of the 96*h* site were fixed at the values derived from $Li_4Nd_3TeSbO_{12}$ due to the weak scattering arising from the low occupancy (0.038(1)) of the this site in $Li_{3.5}Nd_3Te_{1.5}Sb_{0.5}O_{12}$.

The structural characterization of the remaining compositions ($x = 0.05$, 0.1, 0.2, 1.5) proceeded by an analysis of the diffraction data using the same structural model, albeit simplified to deal with the limitations of the lower resolution neutron diffraction data, the weak scattering of X-rays by lithium and the inherent difficulty of studying lithium distribution on a site with exceedingly low occupancy. Because of this low occupancy of the 96*h* site, the coordinates of the lithium at this position were fixed in all these refinements. In addition to this, the lithium displacement parameter was fixed in the refinements against X-ray data and, in the case of $Li_{3.05}Nd_3Te_{1.95}Sb_{0.05}O_{12}$ strong absorption combined with surface roughness led to nonpositive definite displacement parameters as have been observed previously in data collected using the same instrument from related garnets. Therefore the data collected from $Li_{3.05}Nd_3Te_{1.95}Sb_{0.05}O_{12}$ were modeled by fixing the displacement parameters at values derived from the neutron diffraction data collected from $Li_4Nd_3TeSbO_{12}$ and refining an absorption correction.[19] These X-ray diffraction data collected from $Li_{3.05}Nd_3Te_{1.95}Sb_{0.05}O_{12}$ contained two weak Bragg peaks that could not be indexed as arising from any of the reagents or likely products or a garnet phase of reduced symmetry. Due to the high metric symmetry of the garnet, it is probable that the presence of the Bragg peaks from this minor impurity peaks in the diffraction profile have negligible impact on the structural refinement.

The data collected from $x = 0.05$, 0.1, 0.2, and 1.5 were fitted using isotropic displacement parameters and the lithium distribution was refined within the constraint imposed by stoichiometry. In every case a reasonable fit was obtained to the data as illustrated in Figure 3. The resultant fit and

(19) Suortti, P. *J. Appl. Crystallogr.* **1972**, *5*, 325.

Table 1. Fit Parameters and Structural Data for $Li_{3+x}Nd_3Te_{2-x}Sb_xO_{12}$ derived from Rietveld Refinement against X-ray or Neutron Powder Diffraction Data Collected at Room Temperature[a]

	$Li_{3.05}Nd_3Te_{1.95}Sb_{0.05}O_{12}$	$Li_{3.1}Nd_3Te_{1.9}Sb_{0.1}O_{12}$	$Li_{3.2}Nd_3Te_{1.8}Sb_{0.2}O_{12}$	$Li_{3.5}Nd_3Te_{1.5}Sb_{0.5}O_{12}$	$Li_4Nd_3TeSbO_{12}$	$Li_{4.5}Nd_3Te_{0.5}Sb_{1.5}O_{12}$
radiation/ instrument	X-ray/ laboratory	neutron/D1A	neutron/D1A	neutron/Polaris	neutron/Polaris	X-ray/laboratory
a_o (Å)	12.55576(12)	12.5597(9)	12.5602(2)	12.59413(12)	12.62138(12)	12.6253(2)
R_{wp}	3.70	4.04	4.69	2.73	2.29	11.56
χ^2	5.27	1.498	1.386	2.63	2.00	8.34
Li 24*d* occupancy	0.92(4)	1.00(3)	1.00(4)	1.014(4)	0.987(6)	0.87(4)
Li 96*h* occupancy	0.024(9)	0.009(8)	0.017(10)	0.038(1)	0.087(1)	0.158(10)
O *x*	0.2773(5)	0.27732(14)	0.2774(2)	0.27743(2)	0.27772(3)	0.2812(4)
O *y*	0.1063(4)	0.1070(2)	0.1074(2)	0.10694(2)	0.10638(3)	0.1043(4)
O *z*	0.2012(4)	0.2002(2)	0.2000(2)	0.19968(2)	0.19861(3)	0.1998(4)
100 Nd U_{iso} (Å^2)	0.79	0.15(7)	0.15(7)	0.54[b]	0.79[b]	0.52(5)
100 Te/Sb U_{iso} (Å^2)	0.69	0.20(8)	0.07(9)	0.56[b]	0.69[b]	0.07(6)
100 Li U_{iso}/ (Å^2)	1.83	0.9(2)	1.0(3)	1.38(4)	1.83(5)	1.83
100 O U_{iso} (Å^2)	1.01	0.54(6)	0.43(6)	0.83[b]	1.01[b]	0.6(2)

[a] Atomic coordinates: Nd 24*c* $^1/_8$, 0, $^1/_4$; Te/Sb 16[a] 0, 0, 0; Li 24*d* $^1/_4$, $^7/_8$, 0; Li[a] 96*h* 0.1126(13), 0.6599(10), 0.6334(10); O 96*h x, y, z*; [b] U_{iso} equivalent to refined anisotropic values; [c] atomic coordinate refined against Polaris data collected from $Li_4Nd_3TeSbO_{12}$ and fixed for all other compositions.

Table 2. Selected Bond Lengths (Å) for $Li_{3+x}Nd_3Te_{2-x}Sb_xO_{12}$ Derived from Rietveld Refinement against X-ray or Neutron Powder Diffraction Data Collected at Room Temperature

compd[a]	Li(24d)−O × 4	Nd−O × 4	Nd−O × 4	Te/Sb−O × 6
$Li_{3.05}Nd_3Te_{1.95}Sb_{0.05}O_{12}$[b]	1.914(7)	2.411(5)	2.560(5)	1.936(5)
$Li_{3.1}Nd_3Te_{1.9}Sb_{0.1}O_{12}$[c]	1.925(2)	2.421(2)	2.546(2)	1.932(2)
$Li_{3.2}Nd_3Te_{1.8}Sb_{0.2}O_{12}$[c]	1.927(3)	2.426(3)	2.546(5)	1.928(3)
$Li_{3.5}Nd_3Te_{1.5}Sb_{0.5}O_{12}$[d]	1.9302(3)	2.4292(3)	2.5486(3)	1.9409(3)
$Li_4Nd_3TeSbO_{12}$[d]	1.9315(4)	2.4370(4)	2.5419(4)	1.9578(4)
$Li_{4.5}Nd_3Te_{0.5}Sb_{1.5}O_{12}$[b]	1.885(5)	2.462(5)	2.560(5)	1.983(5)

[a] Refined against. [b] X-ray diffraction data, [c] D1A neutron data, [d] Polaris neutron data

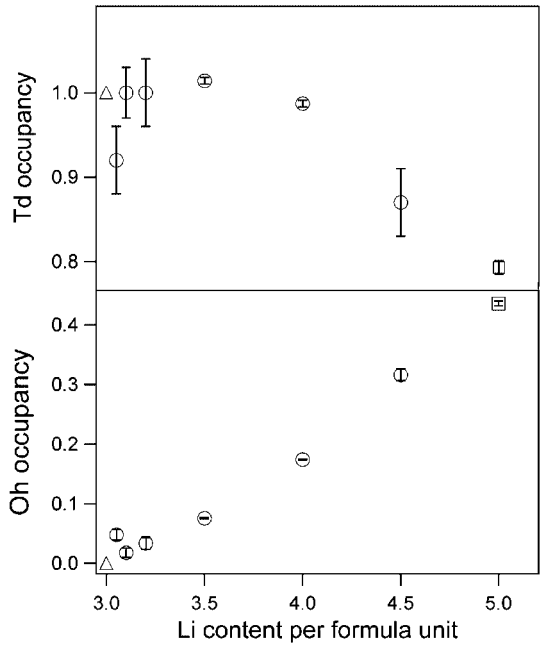

Figure 4. Ooccupancy of the oxide tetrahedra (24 *d*) and octahedra in the series $Li_{3+}Nd_3Te_{2-x}Sb_xO_{12}$ are represented by circles. Occupancies shown by $Li_3Nd_3Te_2O_{12}$ and $Li_5La_3Sb_2O_{12}$ are taken from the literature and are shown by triangles and squares, respectively. The error bars represent one standard deviation derived from the Rietveld refinements and the variation reflects the different diffractometers used to characterise the compounds.

structural parameters are collected in Table 1, selected bond lengths are listed in Table 2, and the lithium distribution is shown in Figure 4.

^{7}Li MAS NMR. The ^{7}Li MAS spectrum of samples of composition $Li_4Nd_3TeSbO_{12}$ and $Li_{4.5}Nd_3$ $Te_{0.5}Sb_{1.5}O_{12}$ are compared with that of $Li_3Nd_3Te_2O_{12}$ in Figure 5 and the ^{6}Li MAS spectrum of $Li_3Nd_3Te_2O_{12}$ is shown in Figure 6. For $Li_3Nd_3Te_2O_{12}$, a single manifold of narrow spinning sidebands is observed in the ^{7}Li spectrum, centered at +10 ppm (reference 1 M LiCl (aq)) and approximately 240 kHz in width. For $Li_{4.5}Nd_3$ $Te_{0.5}Sb_{1.5}O_{12}$, two sideband manifolds are resolved, centered at −3 and 25 ppm, respectively, with similar widths. By comparison with the spectrum of $Li_3Nd_3Te_2O_{12}$ the narrower line at −3 ppm can be assigned to lithium in tetrahedral sites, whereas the broader line at 25 ppm arises from lithium in octahedral sites.

This assignment is supported by their relative intensities in a quantitative spectra recorded with a relaxation delay of 3600 s in which the ratio of tetrahedrally to octahedrally coordinated lithium is 1.37:1 at room temperature, in reasonable agreement with the value of 1.57:1 determined from diffraction experiments. This ratio decreased smoothly as temperature was increased to a value of 0.71:1 at 473 K. The resonances arising from tetrahedrally coordinated lithium are considerably narrower, fwhm = 1.0 kHz, than those due to lithium occupying the oxide octahedra, fwhm = 4.0 kHz. The shifts and the line width of the tetrahedral resonance are independent of temperature, while the line width of the octahedral resonance increases to 6 kHz at 473 K.

Spin–lattice relaxation studies show T_1 relaxation times for the two sites which differ significantly; the octahedral T_1 is some 5 orders of magnitude smaller than that of the tetrahedrally coordinated lithium. The more rapid relaxation of the octahedral site was modeled using a single T_1 component of 8 ms and found to be independent of

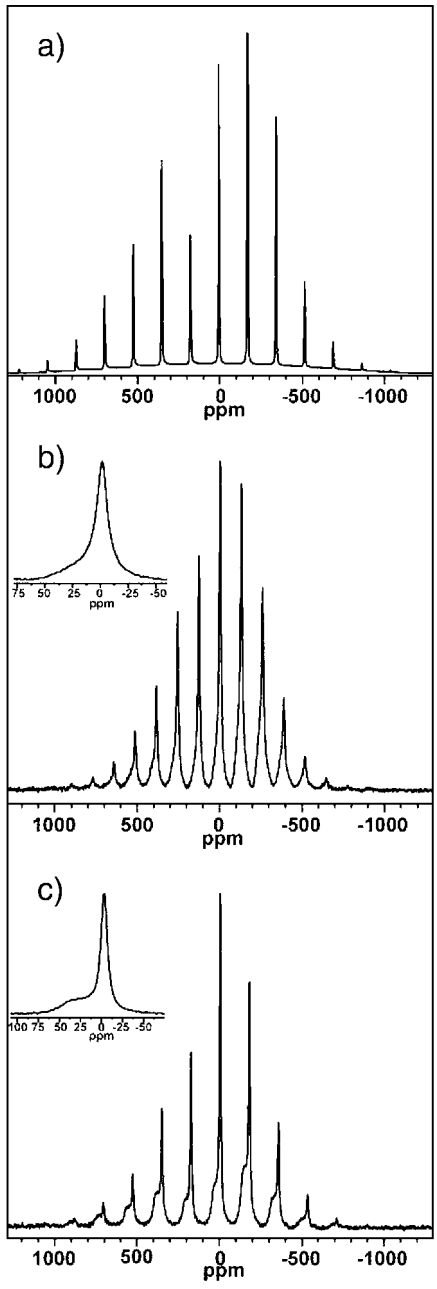

Figure 5. ^{7}Li MAS spectrum of (a) $Li_3Nd_3Te_2O_{12}$ where lithium is exclusively accommodated in tetrahedral interstices and the compounds (b) $Li_{4.0}Nd_3SbTeO_{12}$ and (c) $Li_{4.5}Nd_3Sb_{1.5}Te_{0.5}O_{12}$ containing lithium in a mixture of tetrahedral and octahedral sites. The insets in (b) and (c) show expansion of the centreband.

temperature over the range studied. The slower relaxation of the tetrahedral site could be satisfactorily reproduced using two T_1 components of approximately 15 s and 5 min at room temperature. These values reduced as temperature increased to become 3.5 s and 2 min at 473 K. In the temperature range studied by NMR the resonances from the two lithium sites do not coalesce and the two sites show significantly different spin–lattice relaxation behavior. This suggests that any motion involving tetrahedral to octahedral site exchange is on a time scale longer than milliseconds at temperatures below 473 K.

Impedance Spectroscopy. The electrical impedance was measured as a function of temperature for $x = 0.05$, 0.1, 0.2, 0.5, 1.0, and 1.5 over the range 294 K $\leq T \leq$ 873 K. Impedance data collected from $Li_{3.1}Nd_3Te_{1.9}Sb_{0.1}O_{12}$ are shown in Figure 7 and demonstrate the two arcs with centers depressed below the real axis previously reported in the related fast Li^+ conducting phase $Li_5La_3Ta_2O_{12}$.[6] The observation of two arcs allows the resolution of bulk (intragrain) resistance and grain boundary (intergrain) resistance.

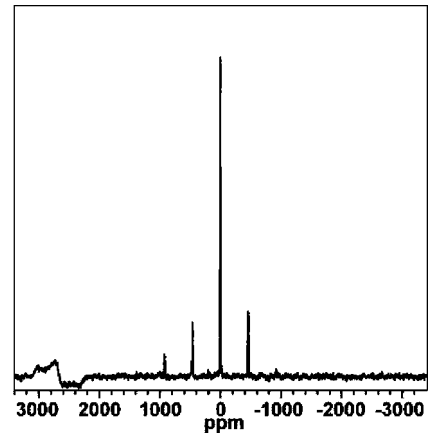

Figure 6. ^{6}Li MAS spectrum of $Li_3Nd_3Te_2O_{12}$. Shifts are reported using a 1 mol dm^{-3} LiCl (aq) reference.

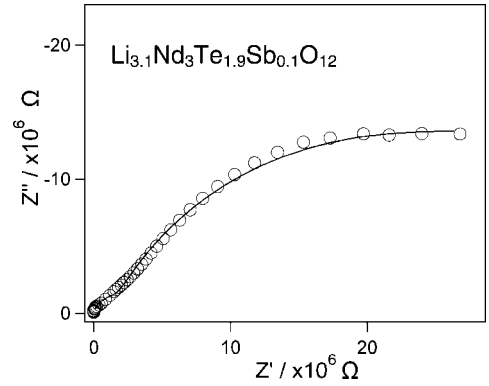

Figure 7. Complex plane plot of the impedance of $Li_{3.1}Nd_3Te_{1.9}Sb_{0.1}O_{12}$ at 47 °C. The line represents the fit obtained to the data using an equivalent circuit model consisting of a constant phase element (CPE) in series with two CPE/resistor parallel components.

The data collected from $Li_{3.1}Nd_3Te_{1.9}Sb_{0.1}O_{12}$ at room temperature could be fitted using an equivalent circuit model consisting of a constant phase element (CPE) in series with two CPE/resistor parallel components. The single CPE represented nonideal diffusion occurring between the lithium-blocking plates of the electrodes. The two CPE/resistor components modeled the contribution from migration occurring within and between the grains to give capacitances of 5×10^{-12} and 3×10^{-10} F, respectively. When the temperature was increased it was no longer possible to delineate these two arcs in the complex plane and so the parameters in the equivalent circuit model were underdetermined. Similar observations have been reported for $Li_5La_3Ta_2O_{12}$[6] and $Li_3Nd_3Te_2O_{12}$[13] and the data collected from $Li_{3+x}Nd_3Te_{2-x}Sb_xO_{12}$ were analyzed using the same approach; namely taking the single arc to represent the total impedance of the system and extracting a value for total conductivity from the intercept of this arc with the real axis

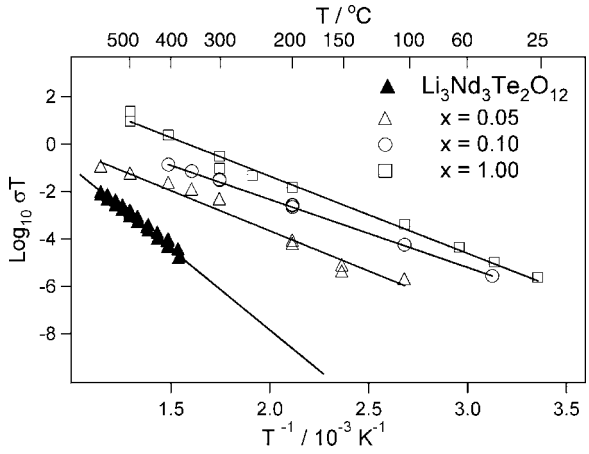

Figure 8. Comparison of the conductivities of selected compositions $Li_{3+x}Nd_3Te_{2-x}Sb_xO_{12}$ and literature values for the conductivity of $Li_3Nd_3Te_2O_{12}$. Lines represent the linear fits to each data set that were used to calculate the activation energy for ionic conduction.

and correcting for the dimensions of the pellet. The values extracted by this method are thus directly comparable with the reported impedances of the compounds $Li_5La_3Ta_2O_{12}$, $Li_6BaLa_2Ta_2O_{12}$, and $Li_3Nd_3Te_2O_{12}$ and provide a robust assessment of the temperature dependence of impedance in the $Li_{3+x}Nd_3Te_{2-x}Sb_xO_{12}$ system.

The absolute values of conductivity extracted via this method depend on; (i) the intragrain resistance, (ii) the intergrain resistance, and (iii) the relative proportions and connectivity between (i) and (ii), i.e., the microstructure of the sample. Although it has been shown in related garnets[7] that the contributions of (i) and (ii) to the conductivity are of the same order of magnitude, in the system $Li_{3+x}Nd_3Te_{2-x}Sb_xO_{12}$ it is not possible to asses the impact of compositional variation on the microstructure. Consequently, the measurement of the overall conductivity underdetermines the different contributions to conductivity and does not provide a precise assessment of the relative intragrain conductivities of different compounds in the series. Nevertheless, the temperature dependence of the conductivity does give an accurate assessment of the activation energy of thermally activated transport in these compounds. The microstructure can have dramatic impact on the physical properties of a material[20] and altering the processing conditions, for example by hot pressing,[21] can lead to a reduction in the grain boundary resistance in ionic conductors. The conductivities reported here, with unoptimised microstructure, should therefore be considered as a lower limit for materials with these compositions. Studies of related garnet systems have shown that microstructural effects can vary the conductivity by an order of magnitude.[22]

Conductivities acquired in this manner from selected compositions in the series $Li_{3+x}Nd_3Te_{2-x}Sb_xO_{12}$ are shown in Figure 8 and compared with the data previously reported for $Li_3Nd_3Te_2O_{12}$. The data collected from all other samples were treated in the same manner and Figure 9 shows the conductivities and activation energies extracted from the

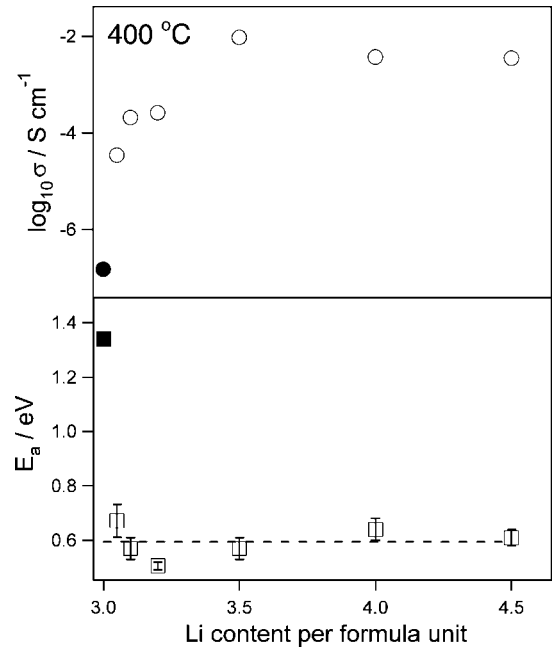

Figure 9. Conductivity at 400 °C (top) and activation energy (bottom) of $Li_{3+x}Nd_3Te_{2-x}Sb_xO_{12}$. Solid symbols represent data for $Li_3Nd_3Te_2O_{12}$. In the lower trace the error bars represent in one standard deviation from the least-squares fit to the Arrhenius plot and the dashed line indicates the mean value of the activation energy for $x > 0$.

Arrhenius plots. The activation energy is rapidly reduced as a function of composition from 1.34(2) eV in $Li_3Nd_3Te_2O_{12}$ to 0.672(6) eV in $Li_{3.05}Nd_3Te_{1.9}Sb_{0.1}O_{12}$. The activation energy shows minimal variation as a function of composition and, as shown in Figure 9, the activation energies for compositions $x > 0$ shows no significant deviation from a mean value of 0.59 eV. All compounds show a conductivity near room temperature, *ca.* 10^{-8} S cm^{-1}, that provide a sharp contrast to $Li_3Nd_3Te_2O_{12}$ which showed immeasurably small conductivity below 400 °C. The conductivities of the compounds $Li_{3+x}Nd_3Te_{2-x}Sb_xO_{12}$ series are compared at 400 °C and, as shown in Figure 9, clearly shows an increase of 2 orders of magnitude on increasing the lithium content by 1.7% from $Li_3Nd_3Te_2O_{12}$ to $Li_{3.05}Nd_3Te_{1.95}Sb_{0.05}O_{12}$. The conductivity increases with lithium content up to $Li_{3.5}Nd_3Te_{1.5}Sb_{0.5}O_{12}$ and then shows a reduction to $Li_4Nd_3Te_{1.0}Sb_{1.0}O_{12}$ and $Li_{4.5}Nd_3Te_{0.5}Sb_{1.5}O_{12}$.

Discussion

Crystallographic Study. The compounds $Li_{3+x}Nd_3Te_{2-x}Sb_xO_{12}$ all crystallize in the space group $Ia\bar{3}d$ and are part of a continuous solution with the garnet $Li_3Nd_3Te_2O_{12}$ representing one end member. The other compositional limit is given by $Li_5Nd_3Sb_2O_{12}$, which has been reported to form a distorted garnet in the space group $I2_13$.[17] Although we were unable to prepare a phase pure garnet of this stoichiometry, the observation of $Ia\bar{3}d$ symmetry for both the solid solution up to $Li_{4.5}Nd_3Te_{0.5}Sb_{1.5}O_{12}$ and the closely related compound $Li_5La_3Sb_2O_{12}$ suggests that the symmetry of $Li_5Nd_3Sb_2O_{12}$ is most likely $Ia\bar{3}d$ and has previously been underestimated. These compounds contain Nd^{3+} on the square antiprismatic sites and a mixture of Te^{6+} and Sb^{5+} on the octahedral sites conventionally occupied in

(20) Meyers, M. A.; Mishra, A.; Benson, D. J. *Prog. Mater Sci.* **2006**, *51*, 427–556.
(21) Demetry, C.; Shi, X. L. *Solid State Ionics* **1999**, *118* (3–4), 271–279.
(22) Thangadurai, V.; Weppner, W. *J. Solid State Chem.* **2006**, *179* (4), 974–984.

the garnet structure. The bond lengths in this series show that the chemistry of Te, Sb and Nd is similar to that observed in $Li_3Ln_3Te_2O_{12}$ and $Li_5La_3Sb_2O_{12}$.

The lithium distribution in garnet phases is difficult to determine from X-ray diffraction due to the weak scattering from Li^+. Previous neutron diffraction studies have shown that in $Li_3Nd_3Te_2O_{12}$[13] and $Li_3Nd_3W_2O_{12}$,[15] which follow the conventional stoichiometry, the lithium fully and exclusively occupies the tetrahedral site but that for lithium-rich phases such as $Li_5La_3M_2O_{12}$ (M = Ta, Nb, Sb) this site is ca. 80% occupied with the excess lithium occupying oxide octahedra. The lithium content in $Li_{3+x}Nd_3Te_{2-x}Sb_xO_{12}$ is intermediate between these two limits. The collection of high resolution neutron diffraction data from $Li_{3.5}Nd_3Te_{1.5}Sb_{0.5}O_{12}$ and $Li_4Nd_3TeSbO_{12}$ has provided a precise model of the lithium distribution in these compounds. In both of these compounds the lithium distribution across the octahedral and tetrahedral sites shows a smooth, slightly nonlinear, evolution with the lithium content.

The lithium cations that occupy the tetrahedra are precisely located and provide a contrast with the large positional disorder manifested in the presence of two crystallographically equivalent lithium positions in the mostly vacant, heavily distorted octahedral site. This difference in behavior reproduces observations in related phases[10,14] where an isotropic model of lithium disorder led to displacement parameters that could not be rationalized as representing harmonic thermal motion about a single position. It has been shown that this disorder arises from a displacement of the lithium from the center of the octahedron away from a shared oxide face to reduce the lithium−oxide bond length and increase the distance between Li^+ in oxide tetrahedra and octahedra linked by a shared face.[14] The structural analysis of $Li_4Nd_3TeSbO_{12}$ is unique in the $Li_{3+x}Nd_3Te_{2-x}Sb_xO_{12}$ series in permitting refinement of this lithium position. It is noteworthy that even for this composition this site remains mostly vacant and the ability of the neutron scattering experiment to identify the lithium position for this composition is an indication of the high quality of the data. The structures of these compounds reveal a trend of increasing occupancy of the distorted octahedron and decreasing occupancy of the tetrahedral site as the lithium content is increased.

Li^+ Conductivity. All of the structural features of the series $Li_{3+x}Nd_3Te_{2-x}Sb_xO_{12}$ show that the chemistry of this series evolves regularly and provides a link between the poor ionic conductor $Li_3Nd_3Te_2O_{12}$ (σ_{400} $o_C \approx 1.2 \times 10^{-7}$ S cm^{-1}, E_a = 1.25(15) eV) and the fast-ion conducting phases $Li_5La_3Ta_2O_{12}$ and $Li_6BaLa_2Ta_2O_{12}$ (σ_{400} $o_C \approx 1 \times 10^{-1}$ S cm^{-1}, E_a = 0.40 and 0.56 eV, respectively). As $Li_3Nd_3Te_2O_{12}$ contains lithium exclusively on the tetrahedral coordination site it was previously speculated[13] that the large activation energy in this compound may be associated with lithium hopping off this site into a vacant neighboring oxide octahedron and consequently that the tetrahedral position played little direct part in the lithium mobility.

Conductivity measurements on $Li_{3+x}Nd_3Te_{2-x}Sb_xO_{12}$ show that for all compounds the charge transport is determined by a single thermally activated process between room temperature and 600 °C. The activation energy for this process is largely invariant between the different compositions and the mean value of 0.59(6) eV is similar to the values reported for other lithium-rich garnets. The difference between this and the value of 1.25 eV observed for $Li_3Nd_3Te_2O_{12}$ implies the operation of a wholly different mechanism for charge transport. This step-change in the activation energy as a function of composition indicates that the mechanism for high ionic conductivity in the garnets is switched on in a binary manner by any increase of lithium content above three Li^+ per formula unit.

In addition to introducing a different mechanism for charge transport the increase in lithium content causes a large increase in conductivity although the maximum room temperature value of ca. 1×10^{-8} S cm^{-1} in $Li_{3+x}Nd_3Te_{1-x}Sb_xO_{12}$ is considerably smaller than in $Li_5La_3Ta_2O_{12}$ and $Li_6BaLa_2Ta_2O_{12}$. We note that this low conductivity, and the apparent reduction in conductivity despite the increase in carrier concentration on going from $Li_{3.5}Nd_3Te_{1.5}Sb_{0.5}O_{12}$ to $Li_{4.0}Nd_3TeSbO_{12}$, most likely arises from the limitations of the impedance spectroscopy data in resolving the different contributions to the overall conductivity and possible changes in the microstructure. However, it can be noted that ionic mobility in $Li_3Nd_3Te_2O_{12}$ was undetectable below 400 °C and a value of only 5×10^{-7} S cm^{-1} was determined at this temperature and so the impedance data collected from $Li_{3+x}Nd_3Te_{2-x}Sb_xO_{12}$ clearly show that the introduction of less than 2% additional lithium results in an increase in conductivity of 2 orders of magnitude to 4×10^{-5} S cm^{-1} at 400 °C. We note that the much smaller activation energy of $Li_{3.05}Nd_3Te_{1.95}Sb_{0.05}O_{12}$ means that the difference in conductivity between these two compounds at room temperature is anticipated to be several orders of magnitude larger than at 400 °C.

The full occupancy of the eight- and six-coordinate sites in the garnet structure by Nd and Te/Sb means that migrating lithium cations will not be able to occupy either of these sites. Instead the key determinant for the movement of lithium through the $[Nd_3Te_{1-x}Sb_xO_{12}]^{(3+x)-}$ lattice must be either the lithium distribution or the charge distribution of the oxide sublattice. The minimal change in composition between $Li_3Nd_3Te_2O_{12}$ and $Li_{3.05}Nd_3Te_{1.95}Sb_{0.05}O_{12}$ compounds results in similar lattice parameters ($\Delta a = 0.052\%$) and the change in the polarizability of the oxide sublattice due to the introduction of such a low concentration of Sb^{5+} is expected to be minimal. Therefore neither of these effects would be anticipated to substantially influence the mobility of Li^+ through the lattice and cannot be responsible for the large changes in activation energy and conductivity. The observed change in ion mobility must instead arise from the change in lithium distribution between the x =0 and the x > 0 members of this series.

Clearly the introduction of lithium onto the octahedral site in the structure for $x > 0$ is associated with an increase in conductivity of 2 orders of magnitude. It is tempting to conclude from this observation that Li^+ in this coordination environment is responsible for the fast-ion conduction observed in the garnet structure. However, while the presence of vacancies on the tetrahedral sites cannot be established

for low values of x it is clear that in $Li_{4.5}Nd_3Te_{0.5}Sb_{1.5}O_{12}$, a substantial vacancy concentration exists on the tetrahedral site. Such tetrahedral vacancies have been a consistent observation in structural studies of related garnets with larger concentration of lithium cations,[10,14,16] and so it is highly probable that the introduction of octahedral lithium occurs simultaneously with the introduction of vacancies onto the tetrahedrally coordinated position. Consequently caution must be applied in assigning the origin of the lithium mobility as the concentration of octahedrally coordinated lithium and of tetrahedral vacancies are similar (for $Li_4Nd_3TeSbO_{12}$, 4.2×10^{21} Li_{Oh} cm^{-3} and 1.6×10^{20} vac_{Td} cm^{-3}; for $Li_5La_3Ta_2O_{12}$, 9.9×10^{21} Li_{Oh} cm^{-3} and 2.3×10^{21} vac_{Td} cm^{-3}).

We note that the separation between tetrahedra, ca. 3.9 Å, it too large for lithium migration to occur solely via these sites. While ionic motion must involve the octahedral sites, two very different mechanisms for ionic conductivity can be readily envisaged (i) lithium occupying an octahedral site hops through the triangular aperture of a shared oxide face into a vacant tetrahedral site and then into one of the other three octahedra that share faces with each tetrahedron and (ii) lithium hops directly from one octahedron through the gap between a pair of oxide anions into one of the neighboring octahedra that are linked via shared edges. Observations in $Li_3Nd_3Te_2O_{12}$, where Li^+ is only found on the filled tetrahedral position, indicate that there is a considerable barrier to hopping out the highly symmetrical oxide tetrahedron, with an activation energy of at least 1.25 eV. For garnets with >3 Li^+ per formula unit the occupational disorder of both the oxide tetrahedron and octahedron is likely to introduce local strain that may destabilize the lithium in the tetrahedral site and thus reduce the energetic barrier for Li^+ to hop out of the tetrahedron. However, the activation energy is halved on changing the composition from $Li_3Nd_3Te_2O_{12}$ and $Li_{3.05}Nd_3Te_{1.95}Sb_{0.05}O_{12}$ and it is probable that the relatively modest activation energy observed in the latter is insufficient to overcome the energy barrier to Li^+ migration out of the tetrahedron and that this smaller energy barrier is related to direct transfer between the oxide octahedra; i.e. (ii) should be considered to be the much more likely mechanism than (i). This observation finds support in the local information that can be extracted from ^7Li NMR measurements.

^{7}Li MAS NMR. The sideband manifold observed for $Li_3Nd_3Te_2O_{12}$, $Li_4Nd_3TeSbO_{12}$ and $Li_{4.5}Nd_3Te_{0.5}Sb_{1.5}O_{12}$ originates from the dipolar interaction with the electronic moments localized on neighboring Nd^{3+} centers ($^4I_{9/2}$). The reduced width of the manifold observed for ^6Li and the virtually complete absence of a similar ^7Li sideband pattern in the isomorphous diamagnetic compound[23] $Li_3Y_3Te_2O_{12}$ corroborate this interpretation. On the other hand the resonance shift of the centerband arises from a hypertransferred Fermi contact interaction. These shifts are 1–2 orders of magnitude smaller than the variation observed in paramagnetic spinels and rock salt manganates.[24] In the latter a contact interaction arises as a result of transfer of spin density from the *d*-orbitals of Mn^{3+}/Mn^{4+} into the 2*s* orbital of Li^+ via shared oxide anions. In $Li_{3+x}Nd_3Te_{2-x}Sb_xO_{12}$ the paramagnetic center, Nd^{3+} contains three unpaired electrons in the relatively withdrawn 4*f* orbitals and so any spin transfer to Li^+ must be mediated by excitation into the empty 5*d* orbitals. This excitation will greatly reduce the probability of spin transfer and is responsible for the relatively small chemical shifts observed in $Li_{3+x}Nd_3Te_{2-x}Sb_xO_{12}$.

Comparison of $Li_{4.5}Nd_3Te_{0.5}Sb_{1.5}O_{12}$ with $Li_3Nd_3Te_2O_{12}$ shows that the narrow resonances are due to the tetrahedrally coordinated lithium and the broad peaks must therefore arise from the lithium occupying the distorted oxide octahedron. The relative ratios of these two signal agrees well with the crystallographically determined population of these two sites at room temperature. On increasing the temperature the signal arising from tetrahedrally coordinated lithium decreases relative to the octahedral signal. Variable temperature neutron diffraction studies of the related phases $Li_5La_3Ta_2O_{12}$ and $Li_6BaLa_2Ta_2O_{12}$[10] have shown minimal change in lithium site occupancies between 2K and 873 K and the Arrhenius behavior of the ion transport properties of $Li_{3+x}Nd_3Te_{2-x}Sb_xO_{12}$ suggest the carrier concentration is largely temperature independent. The observation of temperature dependence in the intensity of the ^7Li spectra in these compounds is thus unexpected and will be probed further using variable temperature diffraction to assess the lithium distribution at elevated temperature.

The two lithium sites in $Li_{4.5}Nd_3Te_{0.5}Sb_{1.5}O_{12}$ show a difference in relaxation times with lithium occupying the octahedral site relaxing ca. 1×10^5 more rapidly than the tetrahedral site. Similarly, the absence of coalescence indicates that there is no exchange of lithium ions between these two environments on a millisecond time scale. We note that this does not rule out the possibility that lithium ions might hop from octahedral site to octahedral site via a very short residence on an tetrahedral site. However, the high activation barrier to Li^+ movement out of the full tetrahedra in $Li_3Nd_3Te_2O_{12}$ and the absence of exchange in the NMR data both indicate that lithium found on the equilibrium tetrahedral position is immobile compared to that in the octahedra. The presence of both occupational and positional disorder on the Li^+ positions within the octahedra and the presence of vacancies on the tetrahedral sites mean that a precise model of the ion migration in this structure must include a large number of possible local cation arrangements. Such complexity, especially in dynamic structures such as fast ion conductors, is beyond the scope of the experimental approach and lithium mobility in the garnet structure must thus be a strong candidate for examination by computer simulation.

Therefore, it can be concluded that the fast ion conductivity observed in the garnets arises exclusively from the lithium ions in the octahedral coordination environment while the tetrahedrally coordinated lithium in $Li_{4.5}Nd_3Te_{0.5}Sb_{1.5}O_{12}$ remain largely immobile as observed in $Li_3Nd_3Te_2O_{12}$. While this tetrahedral lithium does not contribute to the ionic mobility in these compounds, the observation of an activation energy that is invariant with composition and hence tetrahedral site occupancy indicates that the tetrahedral lithium

(23) Powell, A. S.; O'Callaghan, M. P.; Titman, J. T.; Cussen, E. J. Unpublished results.

(24) Grey, C. P.; Dupre, N. *Chem. Rev.* **2004**, *104*, 4493.

does not act in any way to impede the mobility of lithium through the octahedral sites of the structure. The pathway for Li^+ conductivity in the garnet structure is therefore composed of the distorted octahedra shown in Figure 1 which provide a continuous, three-dimensional framework for Li^+ coordination. Ion movement between these octahedra is impeded by a pair of oxide anions that lie almost perpendicular to the lithium-lithium axis. The interatomic spacing of these anions (3.237 Å in $Li_4Nd_3TeSbO_{12}$) is relatively large and clearly permits facile hopping between octahedra. It is likely that increasing this average interatomic separation, increasing the ease of large local displacements of these oxide anions from the mean position and increasing the polarizability of oxide anion will be crucial in optimizing lithium mobility in the garnet structure.

Conclusions

The lithium content of $Li_3Nd_3Te_2O_{12}$ has been incrementally increased by substitution of Sb^{5+} for Te^{6+} resulting in a continuous adjustment of the lithium cation distribution across the tetrahedral and octahedral interstices in the structure. The incorporation of lithium onto the octahedral site occurs simultaneously with the introduction of vacancies onto the tetrahedral site and causes a step-change in the activation energy for Li^+ conduction indicative of a changeover from the low conductivity of $Li_3Nd_3Te_2O_{12}$ to the fast-ion conductivity previously reported for lithium-rich compositions. Lithium NMR shows that the tetrahedral lithium in $Li_{4.5}Nd_3Te_{0.5}Sb_{1.5}O_{12}$ remains precisely located in a the highly ordered arrangement observed in $Li_3Nd_3Te_2O_{12}$ and does not undergo exchange with the lithium occupying the octahedral sites. Taken together, these data provide the first direct evidence that the heavily distorted oxide octahedra provide a pathway for lithium conductivity giving a mobility of lithium on this site that compares well with established fast ion conductors.

Acknowledgment. We are grateful to the Royal Society for the provision of a University Research Fellowship to E.J.C. and to the Universities of Strathclyde and Nottingham for funding and to Dr. R. Smith at Rutherford Appleton Laboratories and Dr. C. Ritter at the Institut Laue Langevin for assistance with the neutron scattering experiments.

Supporting Information Available: Two additional figures and one additional table (PDF). This material is available free of charge via the Internet at http://pubs.acs.org.

CM703677Q